Rapid Generation of Angular Momentum in Bounded Magnetized Plasma

Wouter J. T. Bos,[1,2] Salah Neffaa,[2] and Kai Schneider[2]

[1]*LMFA, UMR CNRS 5509, Ecole Centrale de Lyon–Université de Lyon, Ecully, France*
[2]*M2P2, UMR 6181 CNRS & CMI, Universités d'Aix-Marseille, Marseille, France*

Direct numerical simulations of two-dimensional decaying MHD turbulence in bounded domains show the rapid generation of angular momentum in nonaxisymmetric geometries. It is found that magnetic fluctuations enhance this mechanism. On a larger time scale, the generation of a magnetic angular momentum, or angular field, is observed. For axisymmetric geometries, the generation of angular momentum is absent; nevertheless, a weak magnetic field can be observed. The derived evolution equations for both the angular momentum and angular field yield possible explanations for the observed behavior.

PACS numbers: 52.30.Cv, 47.65.−d, 52.65.Kj

The generation of large coherent structures of the size of the flow domain is a generic feature of two-dimensional (2D) turbulence. Indeed, due to the inverse energy cascade, 2D flows show a tendency to create space filling structures. The nature of these structures and the way they are produced vary from flow to flow. In the context of Navier-Stokes turbulence, the generation of a large-scale domain-filling structure was predicted by Kraichnan [1] and observed in the case of forced turbulence in a periodic domain in which energy condenses at the smallest possible wave number modes [2,3]. In forced wall-bounded flows, this was reproduced numerically [4] and experimentally [5], and it was shown that a large-scale rotating structure emerges, which dramatically reduces the level of the turbulent fluctuations [6].

A similar observation can be made in fusion plasmas, in which the dynamics share many features with 2D flows due to the imposed magnetic field. It is often assumed that in these plasmas, large-scale poloidal structures, called zonal flows, are beneficial for the confinement as they suppress turbulence and shear apart radially extended structures, which are largely responsible for anomalous transport [7–9]. The hereby created transport barriers might play a key role in the transition to an improved confinement state (*H* mode) [10]. In the case of MHD turbulence, the role of rotation was shown to have a similar effect on the flow, reducing the velocity fluctuations and hereby stabilizing the magnetic field [11]. In the present Letter, we will continue the investigation of wall-bounded nonideal MHD. The generation of zonal flows through the absence of charge neutrality will not be addressed (charge neutrality being implied by the one-field MHD approximation). However, MHD allows for an affordable global description of nonuniform magnetoplasmas [12]. The present work could be related to the *L-H* transition through the beneficial effects of large-scale poloidal rotation (which is observed in the present work) on the confinement of the plasma. The present study is also motivated by the obser-

vation that MHD-equilibria in toroidal geometry imply finite flow-fields due to the presence of nonzero viscosity and resistivity [12–14]. In these works, nonideal MHD steady states were investigated in both the limit of small and large viscosity. In each case, it was shown that the steady state contains nonvanishing velocity fields, at odds with classical static equilibria, on which decades of confinement research are based. In the present work, we will not consider steady states, but we will investigate the full nonlinear relaxation of nonideal MHD with nontrivial boundary conditions in two space dimensions. The resistivity and viscosity are nonzero but small, allowing for a turbulent flow. This approach cannot take into account toroidal velocities and nonuniform toroidal magnetic fields and the extension of the present approach to three dimensions constitutes therefore an important direction for further research.

In the case of decaying Navier-Stokes turbulence, it is shown that the self-organization in a periodic domain will lead to a final state, consisting of two, noninteracting, counterrotating vortices [15]. This picture changes however in the presence of no-slip walls. In this case, the flow relaxes to a state with or without angular momentum, depending on the shape of the domain [16–18]. Indeed, in circular domains without initial angular momentum the flow generally relaxes to a state free from angular momentum [19], whereas as soon as the axisymmetry is broken the flow relaxes to a state containing a domain filling structure, containing significant angular momentum [20]. Theoretical progress has been made to explain the phenomenon in the inviscid case, based on a model of interacting vortices [21–23].

In the case of bounded two-dimensional MHD, it is not known, up to now, to which kind of state the flow relaxes, and this will be addressed in the present Letter. We investigate the case in which both the magnetic field and the velocity field cannot penetrate into the walls. The velocity field obeys the no-slip condition at the wall, whereas the

tangential component of the magnetic field can freely evolve, allowing a net current through the domain. We will focus however in the present study on the case in which no net current is initially present.

We start by writing the governing equations. In the present case, we define two angular momenta: a kinetic and a magnetic one,

$$L_u = \int_\Omega \boldsymbol{e}_z \cdot (\boldsymbol{r} \times \boldsymbol{u})dA, \qquad L_B = \int_\Omega \boldsymbol{e}_z \cdot (\boldsymbol{r} \times \boldsymbol{B})dA \tag{1}$$

in which Ω is the flow domain, $\boldsymbol{r}$ the position vector with respect to the center of the domain, and $\boldsymbol{u}$ and $\boldsymbol{B}$ the velocity and magnetic-field vector, respectively. Through integration by parts, these quantities can also be expressed as a function of the stream function $\psi = \nabla^{-2}\omega$ and vector potential $a = \nabla^{-2}j$, respectively, with $\boldsymbol{j} = j\boldsymbol{e}_z = \nabla \times \boldsymbol{B}$ the current density and $\boldsymbol{\omega} = \omega\boldsymbol{e}_z = \nabla \times \boldsymbol{u}$, the vorticity

$$L_u = -2\int_\Omega \psi \, dA, \qquad L_B = -2\int_\Omega a \, dA, \tag{2}$$

in which a and ψ are chosen to be zero at the wall.

A large value of the angular momentum can generally be associated with the presence of a large-scale vortical structure. By analogy, we can anticipate that a large value of L_B corresponds to a large-scale current density structure, and we baptize the quantity L_B angular field. The evolution equations for L_u and L_B can be derived following the procedure described in Maassen [24], by time deriving Eqs. (1) and using the MHD equations

$$\frac{\partial \boldsymbol{u}}{\partial t} + (\boldsymbol{u} \cdot \nabla)\boldsymbol{u} = -\nabla p + \boldsymbol{j} \times \boldsymbol{B} + \nu\nabla^2\boldsymbol{u} \tag{3}$$

$$\frac{\partial \boldsymbol{B}}{\partial t} = \nabla \times (\boldsymbol{u} \times \boldsymbol{B}) + \eta\nabla^2\boldsymbol{B} \tag{4}$$

together with $\nabla \cdot \boldsymbol{u} = 0$ and $\nabla \cdot \boldsymbol{B} = 0$. The pressure is denoted by p, and ν and η are the kinematic viscosity and magnetic diffusivity, respectively. If we write the Lorentz force in the form

$$\boldsymbol{j} \times \boldsymbol{B} = -\frac{1}{2}\nabla B^2 + (\boldsymbol{B} \cdot \nabla)\boldsymbol{B}, \tag{5}$$

we can absorb the first term into the pressure term of the Navier-Stokes equations by introducing the modified pressure $p^* = p + B^2/2$. The $(\boldsymbol{B} \cdot \nabla)\boldsymbol{B}$ term does not induce new terms in the equation for L_u. It vanishes in a similar way as the nonlinear term $(\boldsymbol{u} \cdot \nabla)\boldsymbol{u}$ does, using $\nabla \cdot \boldsymbol{B} = 0$ and $\boldsymbol{B} \cdot \boldsymbol{n}|_{\partial\Omega} = 0$. The equation for L_u becomes

$$\frac{dL_u}{dt} = \nu \oint_{\partial\Omega} \omega(\boldsymbol{r} \cdot \boldsymbol{n})ds + \oint_{\partial\Omega} p^*\boldsymbol{r} \cdot d\boldsymbol{s}. \tag{6}$$

The only difference with respect to the hydrodynamic case [18] is the pressure which is now replaced by the modified pressure p^*. In most fusion plasmas, the quantity $\beta = p/B^2 \ll 1$ to insure confinement, which means that the magnetic part of the pressure dominates. It is important to note that the pressure term in Eq. (6) vanishes in axisymmetric domains. In this work, we therefore consider both a circular and a square domain to analyze the influence of this term.

The derivation of the equation for L_B is analogous to the derivation for L_u. The resulting equation is

$$\frac{dL_B}{dt} = \eta \oint_{\partial\Omega} j(\boldsymbol{r} \cdot \boldsymbol{n})ds - 2\eta I. \tag{7}$$

We observe that there is a term involving the net current I through the domain defined by $I = \int_\Omega je_z dA$. This term is the equivalent of the circulation in the hydrodynamic case, which is zero due to the no-slip walls. The net current is however not imperatively zero as the tangential magnetic field does not vanish at the wall. Nevertheless, a net current will not be generated if it is initially zero, which is the case in the present work.

We performed computations in two different geometries: a square of size $D = 2$ and a circular geometry with a diameter $D = 2.24$. A description of the generation of the initial conditions and the numerical scheme, a spectral method with volume penalization, are given in [25]. The initial velocity and magnetic field consist of correlated Gaussian noise with vanishing cross-helicity $\int_\Omega \boldsymbol{u} \cdot \boldsymbol{B}dA$. The magnetic Prandtl number, ν/η is equal to one. The initial Reynolds number, based on the domain size, is $\sqrt{2E_u}D/\nu$ and yields 1960. The ratio of the magnetic and kinetic energy $E_B/E_u = 2.3$, with $E_u = \frac{1}{2}\int_\Omega |\mathbf{u}|^2 dA$ and $E_B = \frac{1}{2}\int_\Omega |\mathbf{B}|^2 dA$. The resolution of the simulations is 512^2 Fourier modes. In each geometry, 10 runs were performed starting from different statistical realizations with the same initial parameters. The numerical value of a and ψ is not automatically zero at the domain boundary. This is accomplished a posteriori by substracting a constant value at each point in the domain.

In Fig. 1, snapshots of the stream function and vector potential are shown at $t^* = 0.75$, 3, 12 with $t^* = t\sqrt{2E_u(t = 0)}/D$. It can be inferred from (2) that these quantities should give a good visual interpretation of the presence of angular momentum and field. At time-instant $t^* = 0.75$, in which inertial effects are dominant over viscous effects, it is well visible that the velocity field self-organizes into a large domain-filling structure in the square geometry, whereas in the circular geometry, several structures are observed. At $t^* = 3$, a large structure appears also in the magnetic field in the square geometry. At $t^* = 12$, the large-scale velocity and magnetic structures in the square domain are (anti-)aligned. In the circular domain, the tendency to create domain-filling structures is weaker, even though the magnetic field in the circular domain shows some evidence of the formation of a large current structure at $t^* = 12$. To characterize the relaxation of the flows in both geometries, we also show in Fig. 1 the decay of the kinetic and magnetic energy in both domains, as well as the absolute value of the cosine of the alignment angle.
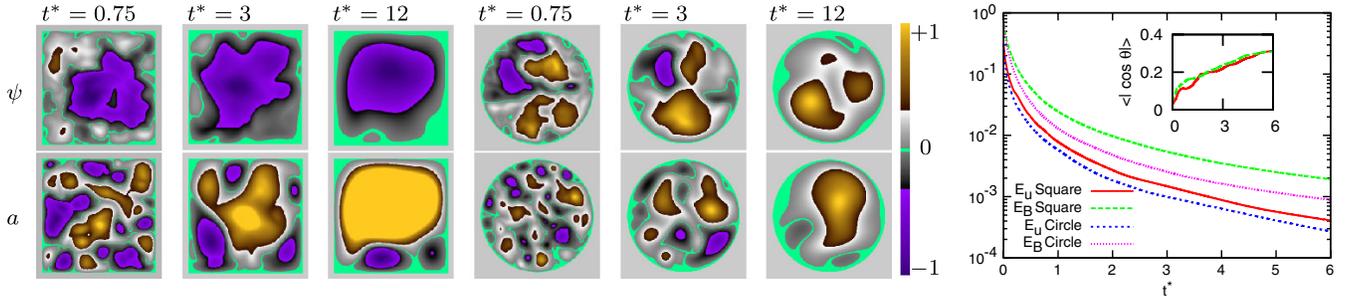
FIG. 1 (color online).   Visualizations of the stream-function ψ and the vector-potential a for both geometries. Figures for ψ are normalized by the maximum of $|\psi|$ (and max($|a|$) for a). The values of max($|\psi|$) are from left to right 0.1, 0.05, 0.03; 0.06, 0.03, 0.01; and for max($|a|$) 0.08, 0.06, 0.04; 0.04, 0.03, 0.01. Right: time evolution of the kinetic and magnetic energy in both geometries. In the inset, the evolution of the absolute value of the relative cross helicity $\langle|\cos(\theta)|\rangle$, illustrates the global alignment of the velocity and magnetic field in both geometries. Solid (red) line: square geometry; dashed (green) line: circular geometry.

A continuous decrease of kinetic and magnetic energy is observed and a continuous increase of global alignment.

At this moderate Reynolds number, spin-up, i.e., spontaneous generation of angular momentum, does not occur in every flow realization. Also, the criterion what is strong or weak spin-up is rather arbitrary. We therefore focus first on mean quantities to illustrate the general tendency to spin-up. In Fig. 2, we show the absolute value of the angular momentum, averaged over 10 runs. We take the absolute value because there is no preferential direction of the spin-up so that an average of the angular momentum would yield values close to zero for all cases. The time evolution of $\langle|L_u|\rangle$ and $\langle|L_B|\rangle$ is shown for both the square and the circular geometry. $\langle\cdot\rangle$ denotes the average over 10 realizations. The quantities are normalized by $\mathcal{L}_u(0) = \|r\|_2\sqrt{2\langle E_u(t=0)\rangle}$ and $\mathcal{L}_B(0) = \|r\|_2\sqrt{\langle 2E_B(t=0)\rangle}$, with $\|r\|_2$ the Euclidean norm of $\mathbf{r}$. The quantity $\mathcal{L}_u(t)$ corresponds to the value of the angular momentum of a flow in solid-body rotation with kinetic energy $\langle E_u(t)\rangle$, which is the flow which optimizes the value of the angular momentum for a given kinetic energy. By analogy, $\mathcal{L}_B(t)$ is used to normalize the angular field. The following is observed: at short times L_u rapidly increases in the square, but does not increase in the circular geometry. The value of L_B also increases in the square, but delayed with respect to L_u. In the circular geometry, an increase of L_B is also observed. In the inset, the values of $\langle|L_u|\rangle$ and $\langle|L_B|\rangle$ are plotted normalized by $\mathcal{L}_u(t)$ and $\mathcal{L}_B(t)$. This normalization has the advantage to correct for the decay of the kinetic and magnetic energy but has the disadvantage that it is sensitive to selective decay [26] so that at long times, we observe generation of angular momentum in each case even if its absolute value might be small. In the following, we will give, where possible, an explanation for the 4 curves in Fig. 2.

First, in the square geometry, a strong spin-up of the velocity field is observed. In the hydrodynamic case, it was argued in [18,20] that the pressure term triggers the spin-up in the square geometry. The magnetic field enhances the pressure term through the magnetic pressure ($p^* = p + B^2/2$). If in the present case it is also the pressure term in

(6) which triggers the spin-up, the effect could be enhanced by increasing the magnetic fluctuation strength B^2. This is illustrated in Fig. 2 (bottom). For one run in which spin-up was observed, the initial magnetic fluctuations are in-
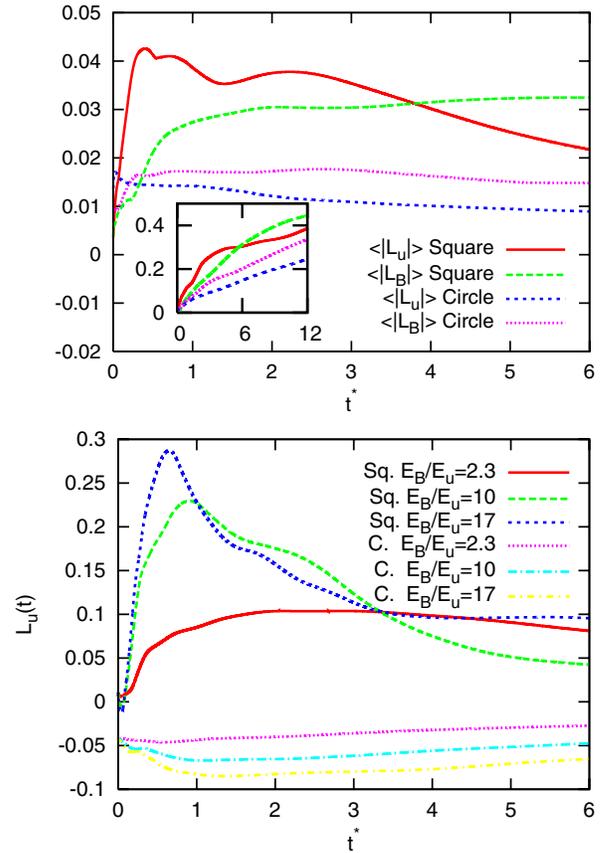
FIG. 2 (color online).   Top: Time evolution of the absolute value of the angular momentum and angular field, averaged over all realizations, normalized by $\mathcal{L}_u(0)$ and $\mathcal{L}_B(0)$, respectively. In the inset, the same quantities are given, normalized by $\mathcal{L}_u(t)$ and $\mathcal{L}_B(t)$ (defined in the text). Bottom: time dependence of the angular momentum L_u in the square and circular geometry, normalized by $\mathcal{L}_u(0)$. The influence of the magnetic pressure on the spin-up in the square container is illustrated by changing the ratio E_B/E_u, while keeping E_u fixed.

creased from $E_B/E_u = 2.3$ up to $E_B/E_u = 10$ and 16.7, while keeping the initial E_u fixed. The resulting spin-up is significantly stronger.

Second, for L_u in the circular geometry, like in the hydrodynamic case [19], no spontaneous spin-up is observed. Increasing the magnetic-field strength does only weakly influence this result (Fig. 2, bottom).

Third, the interpretation of the generation of the angular field in the square geometry is less straightforward, as Eq. (7) does not contain a pressure term. The tendency to create large-scale magnetic structures can be attributed to the selective decay mechanism [27], which was recently shown to persist in bounded geometries [25]. This does however not explain the symmetry breaking or angular momentum generation, which is the main issue of the present work. A possible trigger for the spin-up could be alignment. It is well known that the magnetic field and the velocity field tend to align so that the nonlinear term in the equation for j (or $\boldsymbol{B}$) vanishes. Hence, the magnetic field tends to an alignment with the velocity field which acquired angular momentum through the modified pressure term. It is therefore expected that the magnetic spin-up follows the hydrodynamic spin-up after a time scale corresponding to the alignment. Indeed, L_B spins-up shortly after L_u. The cosine of the angle between $\boldsymbol{u}$ and $\boldsymbol{B}$, measuring the global alignment, is plotted in the inset of Fig. 1 (right). A tendency towards global alignment is observed for long times.

Fourth, in the circular geometry, the weak spin-up of the magnetic field is surprising. Higher resolution simulations are needed to clarify whether this is a viscous effect and/or a statistically more probable (maximum entropy) state. In this context we can refer to [23], where, based on point-vortices, it was shown that two types of most probable states exist in a circular domain: a double vortex, free from angular momentum and an axisymmetric flow, with finite angular momentum. This work neglected the influence of viscosity so that it is not clear how the angular momentum is acquired in the circular geometry.

We now resume our findings. Rapid generation of angular momentum takes place in bounded MHD turbulence, as long as the geometry is nonaxisymmetric. The effect is enhanced by the magnetic pressure. On a slower time scale also, magnetic spin-up is observed in both geometries. It is not clear how this angular field is created. Both alignment and selective decay could be possible explanations.

We want to stress the implications of the present study for confinement research. Fusion plasmas are wall bounded and not axisymmetric so that even in the case of charge neutrality the plasma might have a tendency to create zonal flows and zonal fields, depending on the geometry of the cross-section of the plasma and the strength of the magnetic fluctuations. The present work opens several perspectives for future research, such as the influence of Pr_m, Re, and, in particular, the extension to three dimensions in which the effects of imposed magnetic fields, currents, and toroidal velocities can be taken into account.

[1] R. H. Kraichnan, Phys. Fluids **10**, 1417 (1967).
[2] D. K. Lilly, Phys. Fluids, Suppl. II **12**, 240 (1969).
[3] M. Hossain, W. H. Matthaeus, and D. C. Montgomery, J. Plasma Phys. **30**, 479 (1983).
[4] G. J. F. van Heijst, H. J. H. Clercx, and D. Molenaar, J. Fluid Mech. **554**, 411 (2006).
[5] J. Sommeria, J. Fluid Mech. **170**, 139 (1986).
[6] M. G. Shats, H. Xia, H. Punzmann, and G. Falkovich, Phys. Rev. Lett. **99**, 164502 (2007).
[7] H. Biglari, P. H. Diamond, and P. W. Terry, Phys. Fluids B **2**, 1 (1990).
[8] P. W. Terry, Rev. Mod. Phys. **72**, 109 (2000).
[9] P. H. Diamond, S.-I. Itoh, K. Itoh, and T. S. Hahm, Plasma Phys. Controlled Fusion **47**, R35 (2005).
[10] F. Wagner *et al.*, Phys. Rev. Lett. **49**, 1408 (1982).
[11] X. Shan and D. C. Montgomery, Phys. Rev. Lett. **73**, 1624 (1994).
[12] D. C. Montgomery, J. W. Bates, and L. P. Kamp, Plasma Phys. Controlled Fusion **41**, A507 (1999).
[13] J. W. Bates and D. C. Montgomery, Phys. Plasmas **5**, 2649 (1998).
[14] L. P. Kamp and D. C. Montgomery, Phys. Plasmas **10**, 157 (2003).
[15] G. Joyce and D. C. Montgomery, J. Plasma Phys. **10**, 107 (1973).
[16] S. Li, D. C. Montgomery, and W. B. Jones, Theor. Comput. Fluid Dyn. **9**, 167 (1997).
[17] H. J. H. Clercx, S. R. Maassen, and G. J. F. van Heijst, Phys. Rev. Lett. **80**, 5129 (1998).
[18] H. J. H. Clercx, A. H. Nielsen, D. J. Torres, and E. A. Coutsias, Eur. J. Mech. B, Fluids **20**, 557 (2001).
[19] K. Schneider and M. Farge, Phys. Rev. Lett. **95**, 244502 (2005).
[20] G. H. Keetels, H. J. H. Clercx, and G. J. F. van Heijst, Phys. Rev. E **78**, 036301 (2008).
[21] Y. B. Pointin and T. S. Lundgren, Phys. Fluids **19**, 1459 (1976).
[22] P. H. Chavanis and J. Sommeria, J. Fluid Mech. **314**, 267 (1996).
[23] J. B. Taylor, M. Borchardt, and P. Helander, Interacting vortices and spin-up in 2-d turbulence (to be published).
[24] S. Maassen, Ph.D. thesis, Technische Universiteit Eindhoven, 2000.
[25] S. Neffaa, W. J. T. Bos, and K. Schneider, Phys. Plasmas **15**, 092304 (2008).
[26] G. H. Keetels, Ph.D. thesis, Technische Universiteit Eindhoven, 2008.
[27] W. H. Matthaeus and D. C. Montgomery, Ann. N.Y. Acad. Sci. **357**, 203 (1980).